Journal of Applied Sciences, Information and Computing
Vol. 2, No. 1 (June, 2021)
© School of Mathematics and Computing, Kampala International University

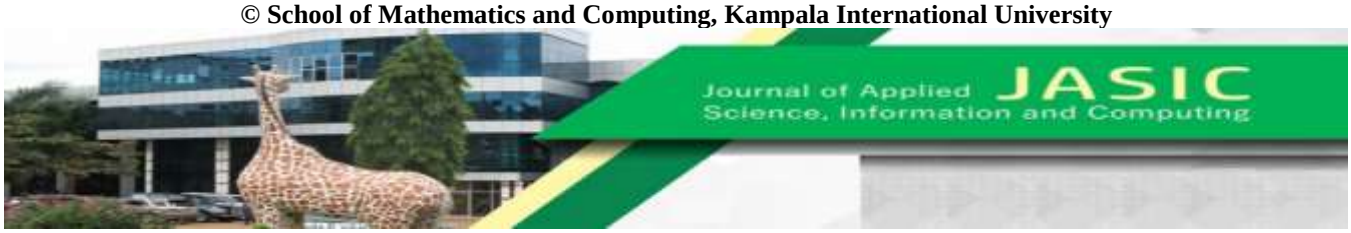

ISSN: 1813-3509 https://jasic.kiu.ac.ug

Dynamics of Heat Generating Upper-Convected Maxwell Fluid in a Porous Medium Over Melting Stretching Sheet with Stratification

A. S. Idowu[1] and J. O. Olabode[2]

[1,2] Department of Mathematics, University of Ilorin, Ilorin, Nigeria.
johnoluwasina34@gmail.com[2], asidowu@gmail.com[2]

Abstract

The flow of heat-generating Upper-Convected Maxwell (UCM) fluid in a porous medium over a melting stretching sheet with stratification is studied. The effects of viscous dissipation, magnetic field, heat generation/absorption, and stratification were considered on velocity, temperature, and concentration. The momentum, energy, and mass distribution models governing the fluid flow are solved numerically via the Spectral Collocation Method. The effects of various pertinent parameters on velocity, temperature, and concentration profiles were presented in graphs and tables. The results reveal that the heat-generating parameter, Eckert number, solutal, and thermal Grashof numbers heighten the velocity field. The temperature of the fluid is geared up with the variational increase in Eckert number and heat-generating parameter. Also, the heat absorption parameter and Eckert number reduce the temperature and concentration boundary layers accordingly.

Keywords: Upper-Convected Maxwell fluid, heat generation, buoyancy effect, stratification, and Spectral Collocation Method.

1. Introduction

Research on non-Newtonian fluids has more applications in industries; thus, it attracts the attention of researchers to propound models fit to represent and answered rheological questions of various classed fluids. Most of the non-Newtonian fluid models; power law and second, and third-grade fluid have been investigated. The second, and third-grade, Walters B model depicts the rheology of fluid whose viscosity is not shear dependent, thus, it is incapable to speculate stress relaxation except elasticity effects of some weakly elastic fluid. The model (power-law model) that estimates shear-dependent viscosity fails to accounts for elasticity effects. However, to estimates for the viscoelastic strength in Maxwell material, (such as plant resin, lubricant, polymers, borax, rubber material, etc) that the theoretical facts may be significant in industry, there is a need for a strong model such as Upper-Convected Maxwell model that will account for stress relaxation and elasticity even for strong elastic material like polymer melt among others. The model has been exploited by various author among which, Alireza, et al. (2018), Kayvan, et al. (2006), Swati, (2012), Bilal, et al. (2017), Omowaye and Animasaun, (2016) have made use of the model to investigate the behavior of the viscoelastic fluid. Some have considered it for both infinite parallel and stretching plates, even at various geometries under magnetic, radiative, suction, and other influences. Some of the findings read that, Upper-Convected Maxwell model can account for the impact of high Deborah numbers in quickly-varying flows experienced in an extremely elastic fluid.

The effect of viscous dissipation becomes imperative to account for energy transportation in fluids when the flow is shear-driven. For instance, fluid flow on a moving plate or stretching sheet (oil between shaft and bearing). The dissipation occurs as a result of the conversion of viscous effect or work done between shear layers irreversibly into the inter-molecular form of energy or internal energy that will raise the temperature of the fluid. Recalling that viscous dissipation is the square of velocity gradient, thus the smaller the distance occupied by the fluid, between the stretching sheet and the other end, the greater the viscous dissipation effect. The interest of various researchers has been geared towards this direction to analyzed this influx on different types of fluid that are practically involved in industrial activities. The effect of viscous dissipation has been studied under free convection flow upon an upright

wavy surface (Alim, et al. 2015). Ajayi, et al. (2017) and Idowu et al. (2020) undertake boundary layer analysis to portray the effects of viscous dissipation and double stratification on MHD Casson fluid flow over a variable thickened surface. Palani and Kim, et al. (2010) discussed the influence of fluid undergoing free convection flow on an inclined semi-infinite variable surface temperature plate. The authors submitted that a substantial increase in temperature distribution is certain with an increase in the magnitude of the Eckert number.

The vast application of Magnetohydrodynamics (MHD) for extrusion of polymer sheet, glass blowing, drawing of plastic films and production of petroleum products, and so on, in metallurgy and chemical engineering processes has become a point of focus to researchers. The cardinal aim of subjecting a flow perpendicular to the magnetic field is to keep the flow laminar by a drag force known as Lorentz force. Several studies had unfolded the attribute of this process on various types of fluid at the different mediums of flow and surface geometry. Among many authors who have worked on this subject are Alireza, et al. (2018) on both analytic and numerical results of Maxwell fluid MHD flow with heat transport analysis, Idowu and Olabode, (2014) on the magnetic field at a various inclination of angles of an unsteady Poiseuille flow while MHD dissipation effects on Casson fluid was studied by Akolade et al. (2021). Other contributing authors on MHD to mention but a few are Subhas, et al. (2012), Shateyi, (2013) and Jabeen, et al. (2020). The summary of the magnetic influence is to economically keep the flow at desirable velocity and boost the temperature of the system owing to the increase in skin friction.

The formation of fluid in different layers engendered by changes in temperature at various levels is referred to as stratification. Its growing effect may lead to severe hypoxia as dissolved oxygen concentration is downgraded. Thus, this practical implication is one of the reasons that triggered the researchers to account for the fluid behavior (changes in fluid properties) for temperature/concentration varying impact at various segments within the flow region. The field observation and statistical analysis of Sebnem, (2008) on water quality in a reservoir is greatly influenced by thermal stratification. Raju, et al., (2107) reported that the concentration and the temperature fields were depreciated with the influence of thermal and solutal stratifications on UCM nanofluid flow with the Cattaneo-Christov heat flux approach. The results of Farooq, et al. (2017) and Mutuku, et al. (2017) note that thermal stratification reduces the fluid temperature, while the solutal stratification downsizes the nanoparticle concentration.

From the existing literature, and to the best of our knowledge, it was observed that the buoyancy, heat generation, and magnetic effects on the case of UCM fluid flow under constant viscosity and thermal conductivity has received no attention. At this juncture, it is worth mentioning that, viscous dissipation effect, ohmic heating, buoyancy effects and some related parameters have not been jointly studied in a stratified porous medium along with the rate of chemical reaction in the boundary layers analysis of UCM fluid. However, to this end, the study is aimed at examining the effect of viscous dissipation, ohmic heating, radiation, and heat source on UCM fluid flow with stratification, and to analyze its usefulness in metallurgical and chemical industries

2. Model formulation

Figure 1 presents the physical model of the problem in a porous medium and the rate of chemical reaction was considered in the mass transfer equation. In this model, the x-axis is taken parallel to the plate direction and the y-axis is normal to it. In view of this, the flow is against gravity (g). It is assumed that the surface is melting and stretching at velocity $U_s = ax$, where $a = U_0 / L$ is the stretching rate. Also, a uniform magnetic field B of strength B_0 is applied perpendicular to the flow direction. The induced magnetic field is neglected with a belief that the magnetic Reynolds number is insignificant. To investigate both heat and mass transfer, $T_s(x) = T_0 + b(x/L)$ and $C_s(x) = C_0 + d(x/L)$ are taken as the prescribed surface temperature and concentration respectively, while $T_\infty(x) = T_0 + c(x/L)$ and $C_\infty(x) = C_0 + e(x/L)$ are the variable free stream temperature and concentration accordingly.

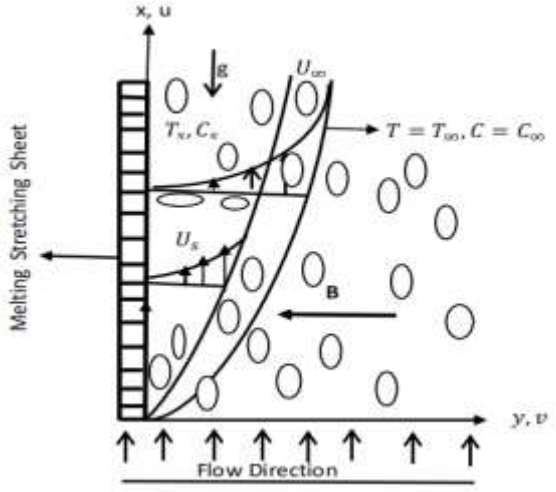

Figure 1: Physical geometry of the flow

Suppose that the fluid temperature and thermal conductivity have a linear relation then the Rosseland approximation for radiation is defined as (Animasaun and Omowaye, 2016).

$$q_r = -\frac{4\sigma^*}{3k^*}\frac{\partial T^4}{\partial y} \quad (1)$$

σ^* is the Stefan-Boltzmann constant, k^* is the Roseland mean absorption coefficient. It is assumed that the temperature difference within the flow is such that T^4 is

expanded in the Taylor series T_s. By discount the higher-order, we have $T^4 \equiv 4T_s^3 T - 3T_s^4$. Thus,

$$\frac{\partial q_r}{\partial y} = -\frac{16\sigma^* T_s^3}{3k^*}\frac{\partial^2 T}{\partial y^2} \quad (2)$$

2.1. Governing Equations

Owing to the above assumptions, the governing equations: continuity, momentum, energy, and concentration representing the UCM fluid flow model are given as :

$$\frac{\partial u^*}{\partial x} + \frac{\partial v^*}{\partial y} = 0 \quad (3)$$

$$u\frac{\partial u^*}{\partial x} + v^*\frac{\partial u^*}{\partial y} + \lambda\left(u^{*2}\frac{\partial^2 u^*}{\partial x^2} + v^{*2}\frac{\partial^2 u^*}{\partial y^2} + 2u^* v^*\frac{\partial^2 u^*}{\partial x \partial y}\right) = \nu\frac{\partial^2 u^*}{\partial y^2} - \frac{\nu}{k_0}\left(u^* + \lambda v^*\frac{\partial u^*}{\partial y}\right) - \frac{\sigma B_0^2}{\rho}\left(u^* + \lambda v^*\frac{\partial u^*}{\partial y}\right) + g\begin{bmatrix}\beta_T(T-T_\infty)+\\ \beta_C(C-C_\infty)\end{bmatrix}, \quad (4)$$

$$u^*\frac{\partial T}{\partial x} + v^*\frac{\partial T}{\partial y} = \frac{k'}{\rho Cp}\frac{\partial^2 T}{\partial y^2} + \frac{Q_0(T-T_\infty)}{\rho Cp} - \frac{1}{\rho Cp}\frac{\partial q_r}{\partial y} + \frac{\mu}{\rho Cp}\left(\frac{\partial u^*}{\partial y}\right)^2 + \frac{\sigma B_0^2}{\rho Cp}u^{*2} \quad (5)$$

$$u^*\frac{\partial C}{\partial x} + v^*\frac{\partial C}{\partial y} = D\frac{\partial^2 C}{\partial y^2} - K_r(C-C_\infty) \quad (6)$$

Equations (3) - (6) are subject to

$$\begin{cases} u^* = 0, k'(\dfrac{\partial T}{\partial y}) = \rho[\lambda^* + c_s^*(T_s - T_0^*)]v^*(x,0), \\ T = T_s(x),\ C = C_s(x) \quad at \quad y = 0 \\ u^* = U_s(x), T \to T_\infty(x), C \to C_\infty(x) \quad as \quad y \to \infty \end{cases} \quad (7)$$

Due to the nature of the fluid and the region of flow, an appropriately modified similarity transformation (following Kayvan, *et al.* (2006), and Swati (2012)) suitable for this work is given as

$$v^* = -\frac{\partial \psi}{\partial x}, u^* = \frac{\partial \psi}{\partial y}, \psi = xu(\eta)(av)^{\frac{1}{2}}, \quad g(\eta) = \frac{T-T_\infty}{T_s - T_\infty}, h(\eta) = \frac{C-C_\infty}{C_s - C_\infty}, \eta = y(\frac{a}{\nu})^{\frac{1}{2}} \quad (8)$$

In this way, the stream function $\psi(x,y)$ identically satisfies the continuity equations (3), as $u^* = \frac{\partial \psi}{\partial y}$ and $v^* = -\frac{\partial \psi}{\partial x}$ respectively. Then, equations (4)-(7) are reduced into dimensionless ordinary coupled differential equations:

$$(1-Ku^2)u''' + (1+2Ku' + KM)uu'' - (u')^2 - (M+Pp)u' + B_t g + B_c h = 0 \quad (9)$$

$$g''(1+Rd) + (\delta - u')\Pr g + \Pr Ek(u'')^2 + \Pr ug' + \Pr(MEku' - A_1)u' = 0 \quad (10)$$

$$h'' + Sc\,uh' - Sc(\alpha + u')h - Sc\,B_1 u' = 0 \quad (11)$$

with dimensionless boundary conditions:

$$\begin{cases} u'(0) = 0, Pru(0) + mg'(0) = 0, g(0) = 0, h(0) = 0, \\ u'(\infty) = 1, g(\infty) = 1 - A_1, h(\infty) = 1 - B_1. \end{cases} \quad (12)$$

Here, $u(\eta)$, $g(\eta)$ and $h(\eta)$ are dimensionless velocity, temperature, and concentration respectively.

Where K= λa, $M = \frac{\sigma B_0^2}{\rho a}$, $Pp = \frac{\nu}{k_0 a}$, $B_t = \frac{g\beta_T L(b-c)}{U_0^2}$ is, $B_c = \frac{g\beta_C L(d-e)}{U_0^2}$, $Rd = \frac{16\sigma^* T_\infty^3}{3k'k*}$, $Pr = \frac{\mu Cp}{k'}$, $\delta = \frac{LQ_0}{a\rho Cp}$, $Ek = \frac{U_s^2}{Cp(T_s - T_\infty)}$, $A_1 = \frac{c}{b-c}$, $B_1 = \frac{e}{d-e}$, $Sc = \frac{\nu}{D}$, $\alpha = \frac{K_r}{a}$, and $m = \frac{(T_\infty - T_0)Cp}{\lambda^* + c_s^*(T_s - T_0^*)}$.

2.2. Engineering parameters

The physical significance parameters of the flow in industries and engineering are skin friction coefficient C_f, local Nusselt number Nu_x, and local Sherwood number Sh_x define as:

$$C_f = \frac{\tau_s}{\rho U_s^2}, Nu_x = \frac{xq_s}{K'(T_s - T_\infty)}, Sh_x = \frac{xJ_s}{D(C_s - C_\infty)} \quad (13)$$

where τ_s, q_s, and J_s are given as

$$\tau_s = [\mu\frac{\partial u^*}{\partial y} - \rho\lambda(2u^* v^*\frac{\partial u^*}{\partial x} + v^{*2}\frac{\partial u^*}{\partial y})]_{y=0}, \quad q_s = -[(K' + \frac{16\sigma^* T_\infty^3}{3k^*})\frac{\partial T}{\partial y}]_{y=0}, \ J_s = -D(\frac{\partial C}{\partial y})_{y=0} \quad (14)$$

by using similarity variable in equation (8):

$$C_f = \frac{1}{\sqrt{Re_x}}[u'' + 2K(u')^2 u - Ku''u^2]_{\eta=0}, \quad Nu_x\frac{1}{\sqrt{Re_x}}(1-Rd)^{-1} = -g'(0), \ Sh_x\frac{1}{\sqrt{Re_x}} = -h'(0) \quad (15)$$

where $\sqrt{Re_x} = \frac{\rho a x^2}{\mu}$ is the local Reynold number.

2.3. Numerical approach and validation of results

To avoid numerical instability as a result of the nonlinear nature of the equations, the Spectral Collocation Method (SCM) is employed to obtain an approximate solution to equations (9)-(11), under the boundary condition in equation (12) (Canuto, *et al.* 1987, Finlayson, *et al.* 1972, and Kayvan, *et al.* 2006).

In this method (SCM), it is assumed that the unknown functions $u(\eta)$, $g(\eta)$ and $h(\eta)$ are approximated as a sum of the basis function $T_n(\xi)$ and the unknown constants, i.e.

$$\left.\begin{aligned} u(\xi) \neg\ u_N(\xi) &= \sum_{n=0}^{N} a_n T_n(\xi) \\ g(\xi) \neg\ g_N(\xi) &= \sum_{n=0}^{N} b_n T_n(\xi) \\ h(\xi) \neg\ h_N(\xi) &= \sum_{n=0}^{N} c_n T_n(\xi) \end{aligned}\right\}, \tag{16}$$

In equation (16), the basis functions are taken as the Chebyshev Polynomials, which are defined in the interval $-1 \le \xi \le 1$ as;

$$T_n(\xi) = \cos(N \cos^{-1}\xi) \tag{17}$$

and $a_n, b_n\ c_n$ are unknown constants to be determined. The domain of definition of the base functions is $[-1,1]$, which is transformed into the domain $[0, L_\infty]$ of flow problem considered by using the transformation

$$\xi = \frac{2\eta}{L_\infty} - 1 \tag{18}$$

thus equation (16) becomes

$$\left.\begin{aligned} u(\eta) \neg\ u_N(\eta) &= \sum_{n=0}^{N} a_n T_n\left(\frac{2\eta}{L_\infty} - 1\right) \\ g(\eta) \neg\ g_N(\eta) &= \sum_{n=0}^{N} b_n T_n\left(\frac{2\eta}{L_\infty} - 1\right) \\ h(\eta) \neg\ h_N(\eta) &= \sum_{n=0}^{N} c_n T_n\left(\frac{2\eta}{L_\infty} - 1\right) \end{aligned}\right\} \tag{19}$$

by substituting equation (19) into equations (9)-(11), non-zero residues were obtained. To minimize error.

$$\int_0^{L_\infty} R(a_n, b_n, c_n, \eta)\delta(\eta - \eta_j)d\eta = R(a_n, b_n, c_n, \eta_j) = 0, \tag{20}$$

$\eta_j \in [0, L_\infty]$, is applied such that residues are close to zero $R(a_n, b_n, c_n, \eta_j) = 0$ at η_j collocation points. Transformed Chebyshev collocation points used as defined by Kayvan, *et al.*, (2006) are.

$$\eta_j = \frac{L}{2}[1 - \cos(\frac{j\pi}{N})],\ j = 0,1,2,...,N. \tag{21}$$

On this note, a system of $3N+3$ algebraic equations with an $3N+3$ unknown coefficient was formed. Newton iteration method (Finlayson, 1972) was used to solve the system of derived algebraic equations to obtain constants $N = 30$. The Mathematical symbolic package used is MATHEMATICA. The obtained values of constants a_n, b_n and c_n are substituted into equation (19), thus, approximate solutions were obtained.

To authenticate the validity of the achieved numerical results, the results obtained by SCM were up to six decimal places correspond to the Runge-Kutta Method used by Animasaun and Omowaye (2016). Both present and published results were compared related to skin friction coefficient $u''(0)$ and local heat transfer rate at the wall $-g'(0)$ in some limiting cases when $\delta = 0$, $K = 0.3$, $A_1 = 0.3$, $M = 0.5$ while Pr and m varies. as shown in Table 1 and 2.

Table 1: Comparison of the numerical result for skin friction coefficient $u''(0)$

Pr	m	Present Study	Animasaun and Omowaye, (2016)
0.3	0	0.0223028	0.0223028
0.7	0	0.0223028	0.0223028
0.3	0.5	0.0146911	0.0146914
0.7	0.5	0.0204999	0.0204998

Table 2: Comparison of the result for local heat transfer rate at the wall $-g'(0)$

Pr	M	Present Study	Animasaun and Omowaye (2016)
0.3	0	-0.0716717	-0.0716716
0.7	0	-0.0344804	-0.0344803
0.3	0.5	-0.0683256	-0.0683261
0.7	0.5	-0.0336168	-0.0336167

3. Results and Discussion

Nonlinear coupled ordinary differential equations (9)-(11) with the boundary conditions in equation (12) have been solved using the Spectral Collocation Method with the aid of MATHEMATICA. The physical properties of the fluid such as thermal conductivity and viscosity are considered non-varying. The numerical simulation was carried out as the default values of parameters $M = m = 0.5$, $Pr = 3.0$, K = B_1 = 0.3, $B_t = B_c = Rd = Pp = 0.1$, Sc = α = A_1 = 0.2, δ = 0.01, Ek = 0.02 unless otherwise stated.

3.1 Effects of relaxation and melting parameters.

Figure 2 depicts the reaction of varying values of K and m on velocity, temperature, and concentration fields. It is shown that the velocity $u'(\eta)$ of the fluid is increased with K (for large relaxation parameter) and has a better improvement with high values of m. This is achieved as

the fluid depicts greater elasticity strength and flow is modeled such that the flow is enhanced by the melting stretching phenomenon on the sheet. However, this influence is significantly noticed towards the free stream. On the other hand, the fluid concentration field is downsized, a degrading temperature distribution occurred towards the sheet but got improved along the free stream.

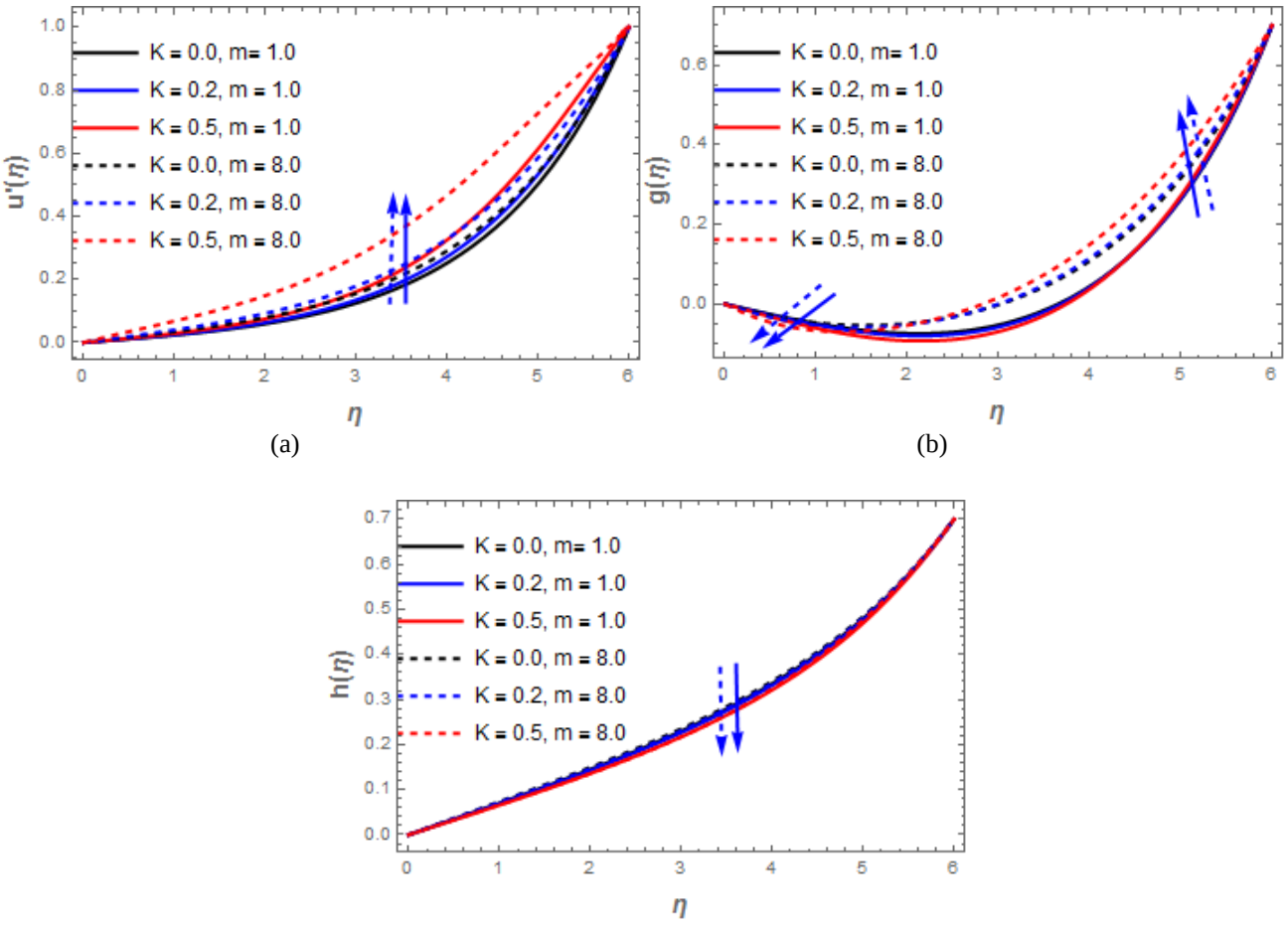

Figure 2: Effects of relaxation and melting parameters (a) velocity, (b) temperature, and (c) concentration profiles

3.2 Impacts of heat generation/absorption parameter and Eckert number

The influence of Eckert number and heat generation/absorption is revealed in figure 3 on the heat energy transportation of the fluid. The effects of viscous dissipation (Eckert number, EK) and heat generation ($\delta > 0$) are to strengthen the temperature distribution of the fluid, while it is seen lowered by $\delta < 0$. Consequently, a maximum heat transfer occurs which helps cool hot surfaces, also generates greater buoyancy force which is important in geophysical flows.

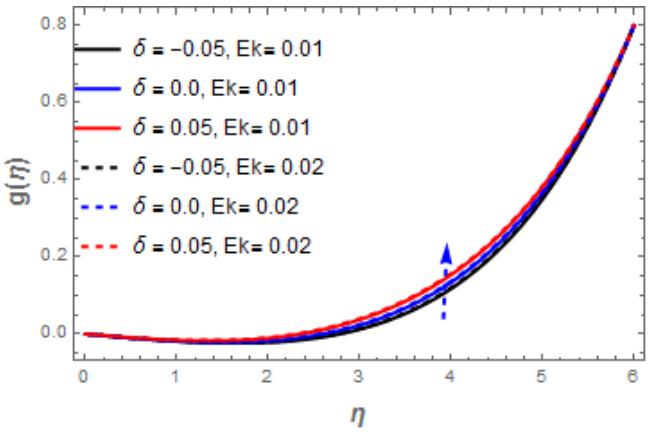

Figure 3: Effects of heat generation parameter and Eckert number on temperature profiles

3.3 Effects of reaction rate parameter and Schmidt number

The account Schmidt number, constructive $\alpha < 0$, and destructive $\alpha > 0$ reaction rate parameters on the fluid transportation are shown in Figure 4. The result shows that it is required to infuse a small Schmidt number to achieve an improvement in molecular diffusion as large values of Sc is found decreasing the velocity field, species, and thermal boundary layers. However, $\alpha < 0$ plays a supportive role to the fluid fields, while $\alpha > 0$ turns around the report. Thus, the conversion of species that occurs as a result of the chemical reaction and thereby reduces concentration boundary layer thickness is linked to the destructive $\alpha > 0$ rate of the chemical reaction.

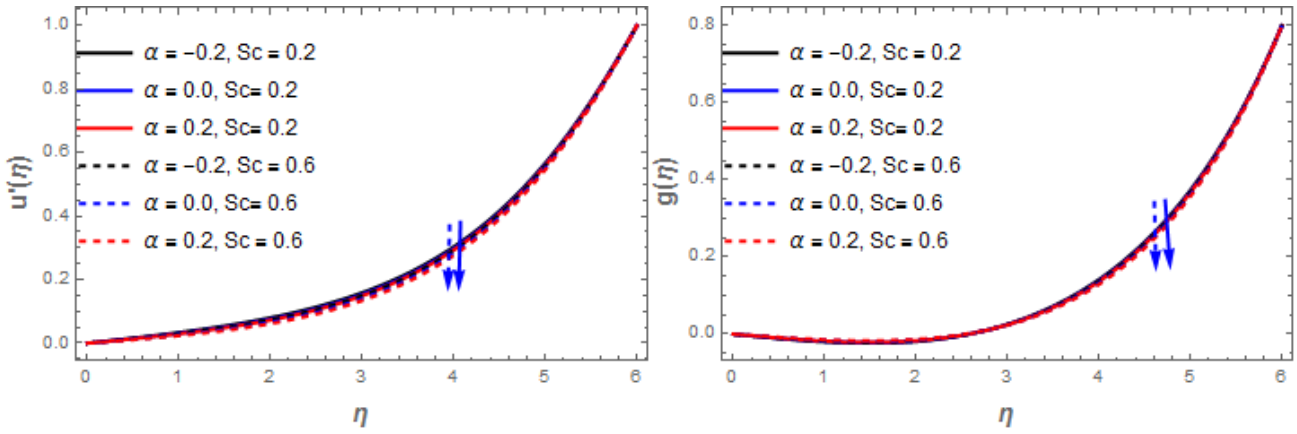

(a) (b)

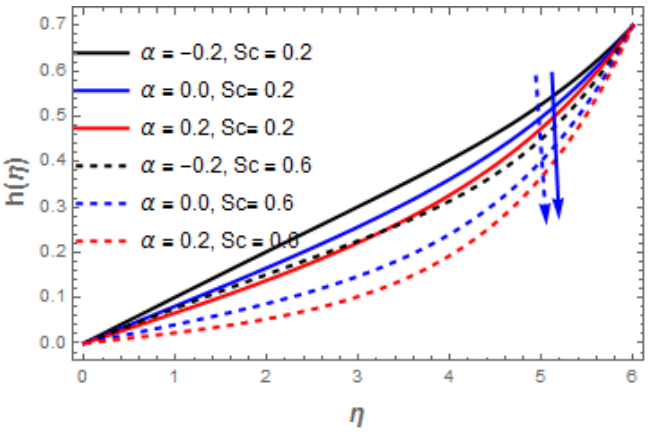

(c)

Figure 4: Effects of reaction rate parameter and Schmidt number (a) velocity, (b) temperature, and (c) concentration profiles

3.4 Effects of magnetic and permeability parameters

In the Figure 5 , an increase in the magnitude of the magnetic parameter retards the velocity of the UCM flow towards the sheet as a result of the Lorentz force generated when the magnetic field is placed to oppose electrically conducting fluid flow. Furthermore, the drag introduced by M engender an increase in the concentration and temperature fields towards the wall and gradually declines along the free stream. In addition, the permeability parameter reduces the velocity, increases the temperature because of the increase in the diffusion of heat as a result of increasing the area of the pore which also gives free passage to the fluid particles.

3.5 Effects of Prandtl number and radiation parameter

The Figure 6 illustrates the impact of Pr and Rd on the temperature field. It is shown that an increase in Prandtl number reduces the temperature. This implies that heat is dispersed faster in the entire region. Also, it is discovered that there is a reduction in the temperature due to the increasing rate of heat transfer via radiation in the flow region. Thus, the heat loss is hopefully minimized and the assessment of the fluid capacity shows that the momentum diffusivity has an edge over thermal transportation

.

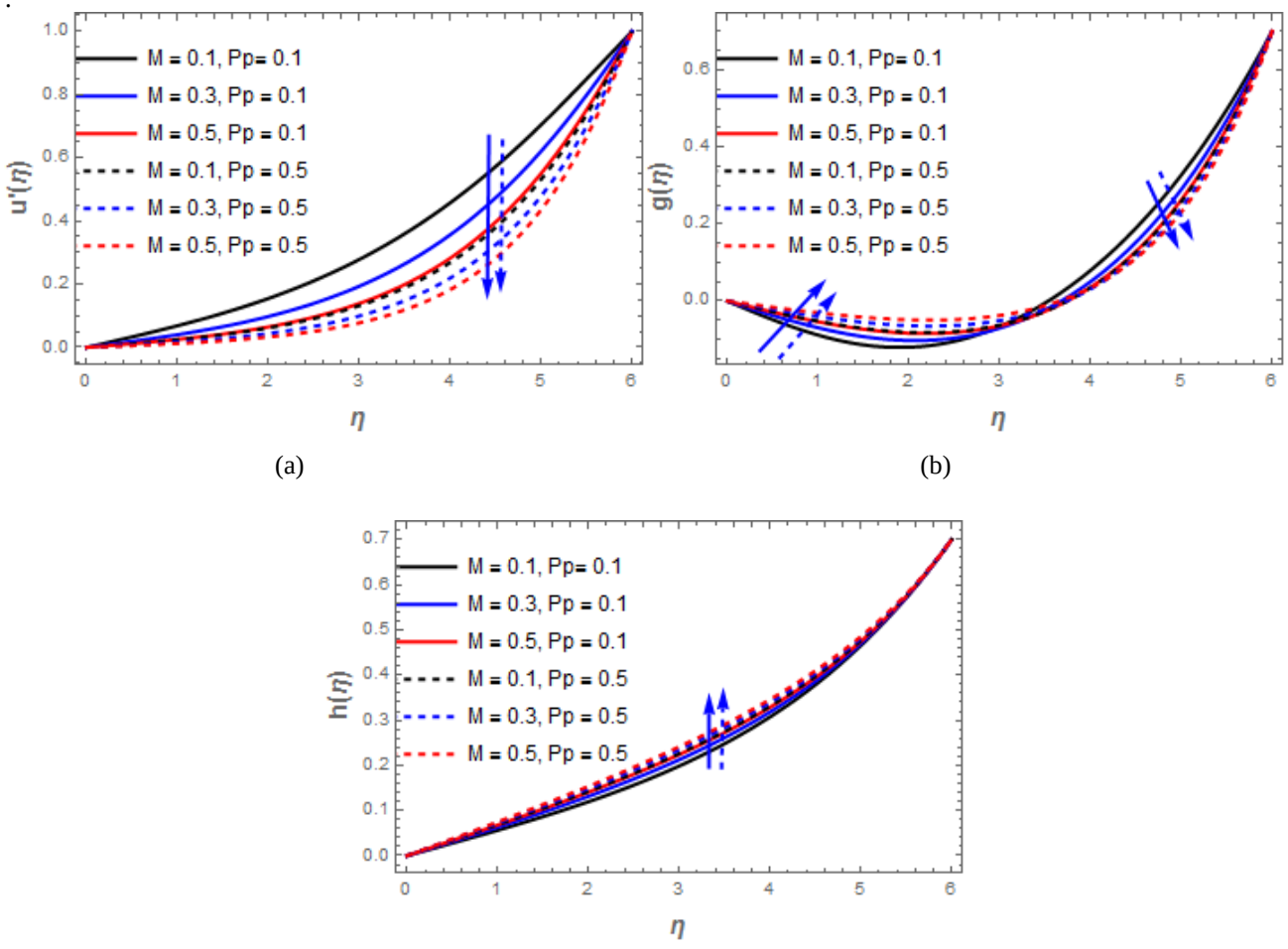

(a) (b)

(c)

Figure 5: Effects of magnetic and permeability parameters (a) velocity, (b) temperature, and (c) concentration profiles

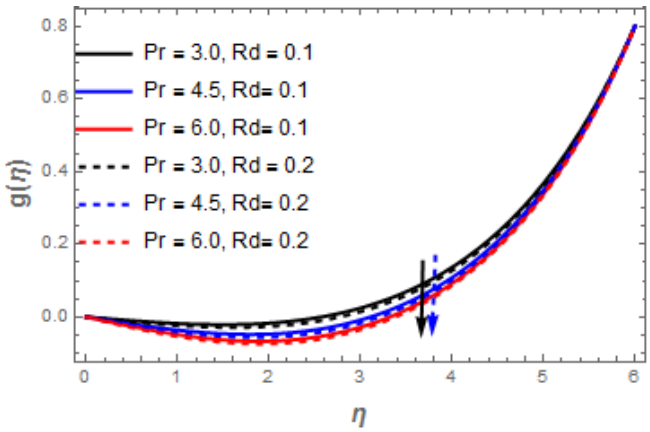

Figure 6: Effects of Prandtl number and radiation parameters temperature profile

3.6 Effects of thermal and solutal Grashof number

The influence of Bt and Bc on the fluid flow is depicted in Figure 7. There is an appreciation in the velocity of the fluid for every mounting value of Bt and Bc. Thus increase in velocity due to the upgrade in thermal boundary force which in turn yields a high rate of heat transfer caused a reduction in the temperature of the UCM fluid.

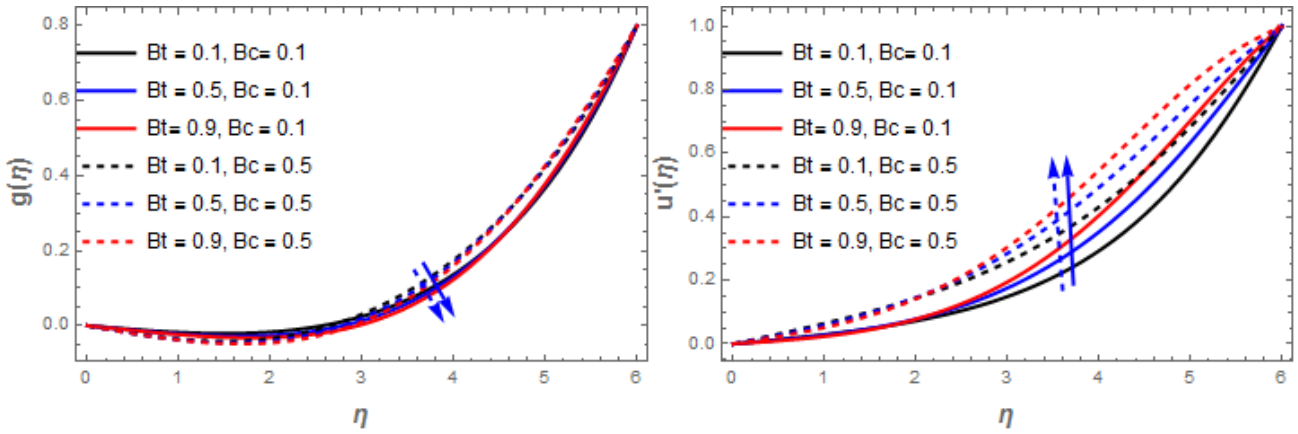

(a) (b)

Figure 7: Effects of thermal and solutal Grashof number (a) velocity and (b) temperature profiles

3.7 Effects of stratification

There is a reduction in the velocity, concentration, and temperature of the fluid with an increasing rate of solutal stratification B_1 as shown in Figure 8. the variation in fluid parcels densities caused by changes in temperature introduces a vertical layering which in turn retards the velocity among others. Thus, the momentum and thermal boundaries are seen decelerating while the concentration profile is appreciated as the magnitude of A increases.

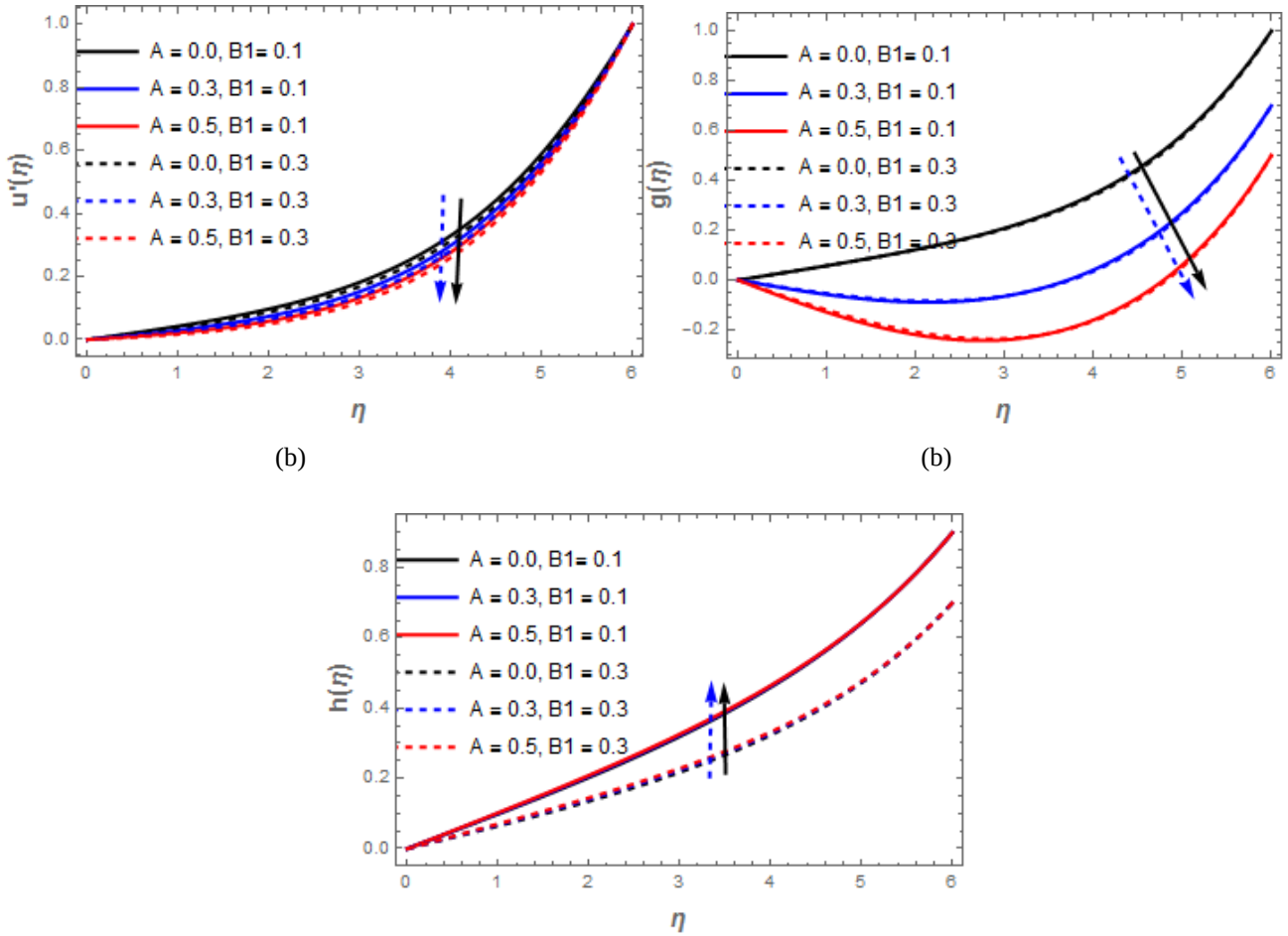

(b) (b)

(c)

Figure 8: Effects of thermal and solutal stratification (a) velocity and (b) temperature and (c) concentration profiles

Table 3: Effects of Sc, Pr, Rd, A **and** $B1$ **on skin friction** $u''(0)$, **Nusselt number and Sherwood number for** $B_t = B_c = 0.1$, $K = 0.3$, $m = 0.5$, $\delta = 0.02$, $Ek = 0.02$, $M = 0.5$ **and** $Pp = 0.1$.

Sc	Pr	Rd	A	$B1$	$u''(0)$	$-g'(0)$	$-h'(0)$
.2	3.0	0.1	0.2	0.3	0.0275738	0.0210933	-0.0663539
.4					0.0239824	0.0186715	-0.0389909
.6					0.0216843	0.0170249	-0.0219295
.2	3.0				0.0275738	0.0210933	-0.0663539
	4.5				0.0255961	0.0406087	-0.0667478
	6.0				0.024245	0.0544108	-0.0669823
	3.0	0.1			0.0275738	0.0210933	-0.0663539
		0.2			0.0270377	0.0267797	-0.0664851
		0.3			0.0264466	0.0332698	-0.0666283
		0.1	0.1		0.0318288	-0.0174201	-0.0651709
			0.3		0.0233291	0.0586057	-0.0675532
			0.5		0.0149646	0.12939	-0.069985
			0.2	0.1	0.032362	0.024423	-0.0993282
				0.3	0.0275738	0.0210933	-0.0663539
				0.5	0.0229001	0.0175546	-0.0346584

Table 4: Effects of K, m, δ, Ek and M on skin friction $u''(0)$, Nusselt number, and Sherwood number for $B_t = B_c = 0.1$, $A = 0.2$, $B_1 = 0.3$, $Sc = \alpha = 0.2$, $Pr = 3.0$, $Rd = 0.1$ and $Pp = 0.1$

K	m	δ	Ek	M	$u"(0)$	$-g'(0)$	$-h'(0)$
.3	0.5	0.0	0.02	0.5	0.0275738	0.0210933	-0.0663539
.5					0.0293659	0.0257548	-0.0638846
.7					0.0499625	0.0356739	-0.0580331
.3	1.0				0.0278788	0.02107	-0.0664136
	3.0				0.0291154	0.0208932	-0.0666486
	5.0				0.0303585	0.0205882	-0.0668745
	0.5	-0.05			0.0272895	0.0210243	-0.0664654
		0.00			0.0275738	0.0210933	-0.0663539
		0.05			0.0280649	0.0191184	-0.0661939
		0.0	0.01		0.0274891	0.0217442	-0.0663792
			0.02		0.0275738	0.0210933	-0.0663539
			0.03		0.0276585	0.0204424	-0.0663285
			0.02	0.1	0.0735739	0.048627	-0.0540508
				0.3	0.0434896	0.033315	-0.0611387
				0.5	0.0275738	0.0210933	-0.0663539

The activities of Sc, Pr, Rd, A and $B1$ on the $u''(0)$, $-g'(0)$ and $-h'(0)$ are depicted in Table 3. The mass transfer at the wall of the fluid is positively influenced while the values of $u"(0)$ and $-g'(0)$ were downsized by $B1$ and Sc accordingly. The reduction in skin friction is helpful in coating processes, yielding an increase in production as the velocity is improved. The increasing values of Pr, Rd and A are supportive to $-g'(0)$ but act contrary against $u"(0)$ and $-h'(0)$. Thus it can be inferred that momentum diffusivity plays actively over thermal diffusion rate. The account of K, m, δ, Ek and M on $u''(0)$, $-g'(0)$ and $-h'(0)$ is revealed in Table 4. The magnitude of Ek and $\delta > 0$ increase the $u"(0)$ and $-h'(0)$, K uphold the values of $u''(0)$, $-g'(0)$ and $-h'(0)$, m only accelerates $u''(0)$, while all the values of $u''(0)$, $-g'(0)$ and $-h'(0)$ are suprssed by M.

4. Summary

The flow of heat-generating Upper - Convected Maxwell fluid in a porous stratified medium on the melting stretching surface was investigated. The flow is against gravity to account for the buoyancy effect and perpendicular to magnetic field strength. The effects of viscous dissipation, Ohmic heating, magnetic field, heat generation, and rate of chemical reaction were considered. A system of coupled ordinary differential equations is derived with boundary conditions by transforming the partial differential equations using similarity transformation variables. The spectral Collocation Method was used to solve the obtained ordinary differential equations. A comparison of the results was made with those existing in the literature and found to be in excellent agreement. The effects of various parameters such as Deborah number, Grashof number, Prandtl number, Eckert number, Schmidt number, permeability, magnetic, radiation, heat generation, reaction rate, and melting parameters on the dimensionless velocity, velocity gradient, temperature, temperature gradient, and concentration are shown below:

a. increase in relaxation and melting parameters enhances the velocity profile;
b. Eckert number and heat generation parameter increase the temperature;
c. magnetic and permeability parameters reduce the velocity, increase the concentration of the fluid throughout the region while the temperature is only improved at some points close to the wall;
d. increase in Prandtl number and radiation parameter reduces the temperature;
e. an increase in reaction rate parameter and Schmidt's number reduce the concentration and velocity of the fluid;
f. increase in Solutal Grashof number and Thermal Grashof number increase the velocity and reduce the temperature of the fluid; and
g. increase in stratification downsized the velocity and temperature but improved the concentration.

5. Conclusions

The results obtained showed that there is a great improvement in the velocity of the fluid which has good important applications in the coating process and extraction industries. Energy loss is reduced due to a reduction in heat transfer at the surface. These will yield improvement in the process and level of production.

- There is maximum heat transfer which is helpful for cooling a hot surface, it also results

to greater buoyancy force which is important in geophysical processes.

- Its viscous dissipation engenders good heat transfer and the flow in porous medium purposefully to diffuse the heat faster is appreciated.

Nomenclature

T	temperature of the fluid
T_0	initial reference temperature
T_s	surface temperature of the fluid
T_∞	ambient temperature
U_0	reference velocity
U_s	stretching sheet velocity
u^*	velocity component along x direction
B	magnetic field
U_0	reference velocity
L_∞	boundary layer edge length
q_r	radiative heat flux
f	dimensionless stream function
c_s^*	solid surface heat capacity
g	acceleration due to gravity
Q_0	internal heat generation
D	mass diffusivity
M	magnetic parameter
B_t	thermal Grashof number
Rd	radiation parameter
A_1	thermal stratification
Sc	Schmidt number
C_f	local skin friction coefficient
Sh_x	local Sherwood number
J_s	surface mass flux
C	concentration of the fluid
C_0	initial reference concentration
C_s	fluid concentration at the surface
C	concentration of the fluid
C_0	initial reference concentration
C_s	fluid concentration at the surface
C_∞	ambient concentration
L	characteristic length
U_∞	free steam velocity
v^*	velocity component along y direction
B_0	magnetic field strength
L	characteristic length
Pr	Prandtl number
k^*	Roseland mean absorption coefficients
k'	thermal conductivity
Cp	fluid heat capacity
k_0	porosity permeability
k_r	chemical reaction rate
K	Deborah number
Pp	permeability parameter
B_c	solutal Grashof number
Ek	Eckert number
B_1	solutal stratification
m	melting parameter
Nu_x	local Nusselt number
q_s	surface heat flux
Re_x	local Reynold number
Greek symbols	
σ^*	Stefan-Boltzmann constants
ψ	Stream function
ρ	fluid density
λ	fluid relaxation time
σ	electrical conductivity
β_T	volumetric thermal expansion
α	reaction rate parameter
η	similarity variable
g	dimensionless temperature
h	dimensionless concentration
ν	dynamic viscosity
δ	heat generation parameter
β_C	volumetric solutal expansion
τ_s	wall shear stress

References

Ajayi, T.M., Omowaye, A.J. and Animasaun, I.L. (2017). Effects of vis cous dissipation and double stratification on MHD Casson. Fluid flow over a

surface with variable thickness: boundary layer analysis, Inter J Eng Research in Africa.; 28:73-89.

Akolade, M.T., Idowu, A.S., and Adeosun, T.S. (2021). Multi-slip and soret-doufur influence on nonlinear convection flow of MHD dissipative casson fluid over a slendering stretching sheet with modified heat flux phenomenon. Heat Transf.;50(4):3913–3933.

Alim, M.A., Kabir, K. H., Andallah, L. S. and Saika M. (1972). Combined effects of viscous dissipation and heat generation on natural convection flow along a vertical wavy surface. Academic Press. New York: 1 - 12.

Alireza R., Morteza A., Iman R., Bengt S., Davood D.G., Mehdi G. (2018). Heat Transfer and MHD flow of non-newtonian Maxwell fluid through a parallel plate channel:analytical and numerical solution. Mechanical Sciences. ;9:61–70. https://doi.org/10.5194/ms-9-61-2018

Bilal, M., Sagheer, M. and Hussain, S. (2017). Three dimensional MHD upper convected Maxwell nanofluid flow with nonlinear radiative heat flux. Alexandria Engineering Journal. http://dx.doi.org/10.1016/j.eaj.2017.03.039.

Canuto, C. Hossaini, M. Y. Quartcroni, A. and Zang, T. A. (1987). Spectral methods in fluid dynamics. Springer. Berlin: 3 - 10.

Farooq M., Javed M., Ijaz K.M., Anjum A., and Hayat T., (2017). Melt ing heat transfer and double stratification in stagnation flow of viscous nanofluid Results in Physics 7:2296–2301.

Finlayson B.A. (1972). The method of weighted residuals and variational principles. Academic Press. New York: 1 - 12.

Idowu A. S., Akolade M. T., Abubakar J. U. and Falodun B. O., (2020). MHD free convection heat and mass transfer flow of dissipative Casson fluid with variable viscosity and thermal conductivity effects J Taibah Univ Sci. 14(1):851–862.

Idowu A. S., Olabode J. O. 2014. Unsteady MHD poiseuille flow between two infinite parallel plates in an inclined magnetic field with heat transfer. IOSR Journal of Mathematics (IOSR-JM).; 10 (3)(2):47–53.

Jabeen, K., Mushtaq, M. and Muntazir, R. M. A. (2020). Analysis of MHD fluids around a linearly stretching sheet in porous media with ther mophoresis radiation, and chemical reaction.Mathematical Problems in Engineering:1 - 14. https://doi.org/10.1155/2020/9685482

Kayvan S., Hadi H., and Seyed-Mohammad T., (2006). Stagnation-Point flow of upper-convected maxwell fluids. International Journal of Non Linear Mechanics. 41:1242 – 1247.

Kayvan S., Hadi H., Seyed-Mohammad T. (2006). Stagnation-point flow of upper-convected Maxwell fluids. International Journal of Non-Linear Mechanics.; 41:1242 – 1247. https://doi.org/10.1016/j.ijnonlinmec.2006.08.005

Khan Z., Rasheed H., Noor S., Khan W., Shah, Q., Khan, I., Kadry, S., Nam, Y., and Nisar K. S. (2020). Analytic solution of UCM viscoelastic liquid with slip condition and heat flux over stretching sheet: The Galerkin approach Mathematical Problems in Engineering. https://doi.org/10.1155/2020/7563693

Mutuku W. N., and Makinde O. D., (2017.) Double stratification effects on heat and mass transfer in unsteady MHD nanofluid flow over a flat surface. Asia Pacific Journal Computational Engineering. 4:2.

Nabila, L., Youb K. B., M'barek, F. and Abdelkader, B. (2015). Vis cous dissipation effect on the flow of a thermodependent Herschelbulkley fluid. Thermal Science; 19(5):1553-1564. DOI:10.2298/TSCI121106080L

Omowaye A. J. and Animasaun I.L. (2016). Upper-convected Maxwell fluid flow with variable thermo-physical properties over a melting surface situated in hot environment subject to thermal stratification. Journal of Applied Fluid Mechanics.; 9(4):1777 – 1790.https://doi.org/10.18869/acadpub.jafm. 68.235.24939.

Palani G. and Kwang Yong Kim. (2010). Viscous Dissipation effects on heat transfer in flow over an inclined plate. J. Appl Mechs and Tech Phy; 51(2):241–248.

Raju, C.S.K., Mahanthesh, B. and Gireesha, B.J. (2017). Cattaneo Christov heat flux on UCM nanofluid flow across a melting surface with double stratification and exponential space dependent internal heat source. Informatic in Medicine.; 23:26-34.http://dx.doi.org/10.1016/j.imu.2017.05.008.

Sebnem Elci. (2008). Effects of thermal stratification and mixing on reservoir water quality. The Japanese Society of Limnology. 9:135–142.

Shateyi, S. (2013). A new numerical approach to MHD flow of a Maxwell fluid past a vertical stretching sheet in the presence of thermophoresis and chemical reaction. Boundary Value Problems; 2013:196

Subhas M. A., Jagadish V. T., MahanteshM. N. (2012). MHD flow and heat transfer for the upper-convected Maxwell fluid over a stretching sheet. Meccanica.;47:385–393.

Swati M. (2012). Upper-convected Maxwell fluid flow over an unsteady stretching surface embedded in porous medium subjected to suction/blowing. Z. Naturforsch.; 67:641-646. https://doi.org/10.5560/ZNA.2012-0075.

Acknowledgment

The authors are sincerely thankful to the University of Ilorin, Nigeria, for providing an accommodating environment for this research interest.